



A new soil degradation method analysis by Sentinel 2 images combining spectral indices and statistics analysis: application to the Cameroonians shores of Lake Chad and its hinterland

Sébastien Gadal, Paul Gérard Gbetkom, Alfred Homère Mfondoum

► To cite this version:

Sébastien Gadal, Paul Gérard Gbetkom, Alfred Homère Mfondoum. A new soil degradation method analysis by Sentinel 2 images combining spectral indices and statistics analysis: application to the Cameroonians shores of Lake Chad and its hinterland. 7th International Conference on Geographical Information Systems Theory, Applications and Management (GISTAM 2021), Apr 2021, Online Streaming, Czech Republic. pp.25-36. hal-03207299

HAL Id: hal-03207299

<https://hal.science/hal-03207299>

Submitted on 24 Apr 2021




HAL is a multi-disciplinary open access archive for the deposit and dissemination of scientific research documents, whether they are published or not. The documents may come from teaching and research institutions in France or abroad, or from public or private research centers.

L'archive ouverte pluridisciplinaire **HAL**, est destinée au dépôt et à la diffusion de documents scientifiques de niveau recherche, publiés ou non, émanant des établissements d'enseignement et de recherche français ou étrangers, des laboratoires publics ou privés.



Distributed under a Creative Commons Attribution - NonCommercial - NoDerivatives 4.0 International License

A new soil degradation method analysis by sentinel 2 images combining spectral indices and statistics analysis: application to the Cameroonians shores of Lake Chad and its hinterland

Sébastien Gadal^{1,4*}^a, Paul Gérard Gbetkom^{1,2}^b, Alfred Homère Ngandam Mfondoum³^c,

1. Aix-Marseille Univ, CNRS, ESPACE UMR 7300, Univ Nice Sophia Antipolis, Avignon Univ, 13545 Aix-en-Provence, France, sebastien.gadal@univ-amu.fr paul-gerard.gbetkom@etu.univ-amu.fr;

2. Laboratory of Botanic, Mycology, and Environment, University Mohammed V Rabat, 1014, 4 avenue ibn battuta Rabat Morocco; elaboudi@gmail.com

3. StatsN'Maps, Private Consulting Firm, 19002 Dallas Parkway, Suite 1536, Dallas, Texas 75287; stats.n.maps.expertise@gmail.com; ngandamh@yahoo.com

4. North-Eastern Federal University, 670000 Yakutsk, Republic of Sakha, Russian Federation

Abstract

This paper aims to model the soil degradation risk along the Cameroonian shores of Lake Chad. The processing is based on a statistical analysis of spectral indices of sentinel 2A satellite images. A total of four vegetation indices such as the Greenness Index and Disease water stress index and nine soil indices such as moisture, brightness, or organic matter content are computed and combined to characterize vegetation cover and bare soil state, respectively. All these indices are aggregated to produce one image (independent variable) and then regressed by individual indices (dependent variable) to retrieve correlation and determination coefficients. Principal Component Analysis and factorial analysis are applied to all spectral indices to summarize information, obtain factorial coordinates, and detect positive/negative correlation. The first factor contains soil information, whereas the second factor focuses on vegetation information. The final equation of the model is obtained by weighting each index with both its coefficient of determination and factorials coordinates. This result generated figures cartography of five classes of soils potentially exposed to the risk of soil degradation. Five levels of exposition risk are obtained from the "Lower" level to the "Higher": the "Lower" and "Moderate to low" levels occupy respectively 25,214.35 hectares and 130,717.19 hectares; the "Moderate" level spreads 137,404.34 hectares; the "High to moderate" and "Higher" levels correspond respectively to 152,371.91 hectares and 29,175.73 hectares.

KEYWORDS: vegetation indices; soil indices; statistics analysis; Lake Chad, Sentinel 2.

1. INTRODUCTION

The state of soil is an important parameter in the monitoring of the land dynamic and exploitation, for sustainable use (Jazouli et al. 2019; Chen et al. 2019). Its degradation, which reduces the exploitation of natural resources in general and restricts the productivity of agricultural soils, causes significant socio-economic impacts. In the far-northern part of Cameroon, the shores of Lake Chad, are in the most exposed zone to the soil degradation risks due to environmental conditions, more severe climatic conditions, and modes of uses and exploitation of natural resources (National Action Plan to Combat Desertification (PAN/LCD) 2006). It is an area marked by degradation and decline of soil fertility, unsuitable cultivation practices, a high extension of barren land, erosion, runoff, and decrease of fallows,

overgrazing, and pesticide pollution (Elias Symeonakis and Drake 2010; GIZ, 2015).

The great spatial and temporal variability of the rainfall combined with the rain aggressiveness constitutes major risks related to the rainfall and accelerates the soil degradation process in this zone (PAN/LCD, 2006). Rainfalls as violent localized showers, and strike bared soils, prepared for sowing and lowly protected or cleaned from their vegetation (Seignobos and Iyébi-Mandjek 2000). This is figured out by the presence of vast expanses of bare soils, most of which are very sensitive to water and wind erosion, accentuated by the dwindling vegetation cover. Slopes are low in this environment, and the level of soil drainage is very varied. It is moreover based on the level of draining that, (Seignobos and

Iyébi-Mandjek 2000) distinguished the well-drained lands (terroir of Makari), the poorly drained, lands with waterlogging (terroir of Bodo-Kouda) and the poorly drained lands with waterlogging and fluvial (terroir of Lake Chad). It is a periodically flooded area, where the main activities are fishing, livestock, agriculture, and trade, shared by a large and varied population coming from at least four neighboring countries (Cameroon, Chad, Niger, and Nigeria), with consequently numerous conflicts.

Several methods are used to quantify and map soil degradation at different spatial and temporal scales. Universal Soil Loss Equation (Wischmeier and Smith 1978) or its modified version (Renard et al. 1997) are used to predict soil erosion. This model depends on the slope, the rainfall, the soil typology, topography, the crop rotation, and the soil conservation practice. Further, (Ali and Saïdati 2003) have used sedimentology and magnetic measurements to identify sediment source areas, assess spatial variations in sediment levels, and classify these zones depending on their degree of spatial reworking. Another method was proposed by Daniel et al, 2018 to map the soil degradation, by collecting field samples and performing an unsupervised Iterative Self-Organizing Data Analysis Technique (ISODATA) classification on the combination of sentinel-2 data image and airborne orthoimages. The United Nations Convention to Combat Desertification quantifies soil organic carbon and extract indicators as soil productivity and land cover using MODIS NDVI data, to map the proportion of land degraded over the world (support by Conservation International, Lund Université, NASA, and Global Environment Facility).

All the above-described methods include several ancillary data and field samples of the study area and need to consider the topography of the field. But the ancillary data are not available in the total to the extent of our study area and the distinct types of soil topology and topography are not easy to distinguish due to the spatial resolution of the image used. So, we need to develop a new remote sensing approach only based, on the soil and the vegetation spectral indices which can allow identifying areas exposed to the risk of soil degradation.

Indeed, remote sensing enables collecting and integrating data for a continuous and repeated observation of the phenomenon on large surfaces (Begni et al. 2005). The reflectance of some objects such as soil and vegetation is a good indicator of changes in the environment (Gbetkom et al. 2018) and can be used to calculate spectral indices useful for the study of soil degradation. Previous models have

been developed on the topic. It is the case of Ngandam et al. (2016) who use the linear and the multiple regressions, and the principal component analyses to assess the status of soil degradation in Far-North Cameroon. Following this last work, the statistical methods will be supplemented in this work by other statistical treatments such as factor analysis, to highlight the level of correlation between the selected indices. Thus, the indices such as the Normalized difference vegetation index (NDVI), Modified Soil Adjusted Vegetation Index (MSAVI2), Normalized Difference Greenness Index (NDGI), Disease water stress index (DSWI) are used in this study to quantify vegetation cover and provide information respectively on chlorophyll activity, the density of vegetation cover, vegetation greenery and plant water stress. On the other hand, soil characteristics are highlighted through spectral indices. Those used for that purpose in this study are moisture stress index (MSI); texture index (TI); colour index (IC); brightness index (BI); cuirass index (CI); topsoil surface particles index (GSI); crusting index (CI); redness index (RI); and salinity index (NDSI).

The mapping of soil degradation from indices is sometimes limited to a simple combination of the index in the form of a band-colored composition (Soufiane Maimouni and Bannari 2011) or to an approach that associates spectral indices with different classification methods (Chikhaoui et al. 2007). On the other hand, (Ngandam et al. 2016), cross indices and model soil degradation by weighting indexes and neo-bands using the coefficient of determination resulting from the linear regression between each index and the weighted sum image. In their approach, (Pandey et al. 2013) cross-spectral indices to land cover maps but, index maps are reclassified according to the level of severity of land degradation and associated with land use and land cover map. Therefore, this paper explores another modeling approach to assess soil degradation. Specifically, in three steps, it highlights soil properties through spectral indices. After that, it proceeds to a statistical analysis of the indices contents to withdraw their correlation trends. Finally, the two steps above propose an overall model to predict soil degradation risk.

2. METHODOLOGY

2.1. The study area: Cameroonian part of lake Chad and hinterland

The study area is located in the Far north administrative region of Cameroon and shares borders with the Republic of Chad to the north and east, the Federal Republic of Nigeria to the west, and the rest of the country to the south (Figure 1). It is located between latitude 12 °N to 13 °N and meridian 14 °E to 15 °E. It is a semi-arid region with a Sudano-Sahelian climate, characterized by a rainy season from June to October and a dry season that runs from November to May. The annual rainfall totals around 400 mm, the temperature range is 7.7 °C, and the average monthly temperature is 28 °C.

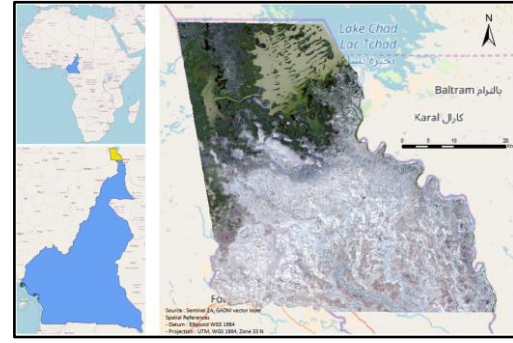


Figure 1: Localisation of the study area

2.2. An approach based on sentinel 2 images

Two Sentinel 2 satellite images acquired on April 29, 2017, were used. They have 13 bands, but only six of them were staked, i.e., Bands 2, 3, 4, 8, 11, and 12.

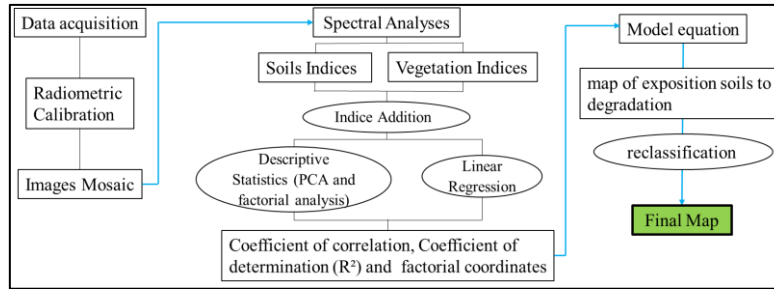


Figure 2: Flowchart of the methodology

2.3. Soil risk of degradation model design

2.3.1. Indices modeling

a. the vegetation index's

The use of vegetation indices has several objectives, such as the estimation of the green vegetable mass, the forecast of harvests, the description of the phenological state of the soil cover, the inventory of

crops by segmentation of indices, and the evolution of vegetation cover at the continental scale (Caloz and Collet 2011). For example, the ability of the NDVI to detect the presence, density, and condition of vegetation was successfully used by Eklundh and Olsson 2003, to observe a greening of the Sahel between 1982 and 2003, due to the spatial increase in vegetation cover. The following indices were therefore used in this study to analyze the chlorophyll activity, the density of vegetation cover, the vegetation greenery, and plant water stress.

Table 1: Characteristics of the vegetation indices

Indices	Algorithm	Goal	References
For the chlorophyll activity: NDVI	$NDVI = (NIR - R) / (NIR + R)$ (Rouse et al. 1973)	Used to evaluate the chlorophyll activity of plants and also for the monitoring of the state of the vegetation cover.	(Martín-Sotoca et al. 2018); (E. Symeonakis and Drake 2004); Pang et al. 2017; (Farooq Ahmad 2012).
For the density of vegetation cover: MSAVI2	$MSAVI2 = \frac{2NIR + 1 - \sqrt{(2NIR + 1)^2 - 8(NIR - R)}}{2}$ (Qi et al. 1994)	Description of the vegetation density and reduces the effects of soil, in particular when the canopy is sparse especially in arid and semi-arid environments.	(Qi et al. 1994); (Ngandam et al. 2016); (Farooq Ahmad 2012).
For the characterization of	$DSWI = (NIR+G) / (SWIR+R)$		

the plant water stress: DSWI	(Apan et al. 2003)	Used to describe the variation of the water content of foliage.	Pu 2008; X. Li et al. 2014; Apan et al. 2003.
For the recognition of the vegetation greenery: NDGI	$NDGI = (G-R) / (G+R)$ (Chamard et al. 1991)	Used to estimate the biomass of vegetation and measure the hydric potential of the leaves at the level of the canopy	(Romero et al. 2018); (Gao et al. 2017); (H. Li et al. 2015); (Rallo et al. 2014); (Sun, Li, and Li 2011).

The visual comparison of vegetation index's efficiency to discriminate and quantify canopy density shows a more accurate representation using MSAVI2. Unlike the NDVI, the MSAVI2 offers a sensitive distinction between bare soils and green areas in less vegetated regions. Also, this index attributes low values to aquatic spaces in contrast to the DSWI and NDGI indices. These observations are consistent with the results of previous works that showed the potential of MSAVI2 to map the state of the vegetation cover in arid environments (Ngandam et al. 2016); (Farooq Ahmad 2012). The four indices distinguish vegetated areas from bare soils. However, the use of soil indices in addition to vegetation indices is essential to characterize the bare spaces. So, nine soil indices are computed and combined.

Table 2: Characteristics of the soil index's

Indices	Algorithm	Goal	References
The moisture stress: MSI	$MSI = SWIR1/NIR$ (Yongnian et al, 2004)	Used to evaluate the spatial extend of less soil moisture, due to the higher level of evapotranspiration.	(Elhag and Bahrawi 2017) ; (Welikhe et al. 2017).
The texture analysis: TI	$TI = (SWIR1 - SWIR2)/(SWIR1 + SWIR2)$ (Madeira Netto 1991)	The texture index is calculated to evaluate the content or percentage of sand, silt, and clay in soil composition, and appreciate the level of the mineral alteration of rock.	(Madeira Netto 1991); (Oliveira et al. 2016); Houssa et al, 1996.
The soil color: CI	$CI = (R-V) / (R+V)$ (Escadafal and Huete 1991)	This index is used to extract information concerning the organic matter content and mineralogical composition of the soil.	(Soufiane Maimouni and Bannari 2011).
The soil brightness: BI	$BI = \sqrt{PIR^2 + R^2}$ (Kauth and Thomas 1976)	The role of the brightness index is to identify the reflectance of soil and to highlight the vegetal cover of bare areas.	(Bannari et al. 1996); (Soufiane Maimouni and Bannari 2011).
The soil Cuirass: CI	$CI = 3 * G - R - 100$ (Pouchin 2001)	It aims is to dissociate vegetated coverings from mineralized surfaces.	Okaingni et al. 2010; Stéphane et al. 2016.
The Topsoil Grain Size: GSI	$GSI = (R-B)/(R+V+B)$ (Xiao et al. 2006)	GSI or topsoil grain size index is an index appropriated to characterize the texture of the soil surface depending on the soil reflectance curve.	(Jieying Xiao, Shen, and Ryutaro 2014); (Ngandam et al. 2016).
The soil crusting: CI	$CI = (R - B) / (R + B)$ (Karnieli 1997)	Is used to detect and map from satellite imagery different lithological morphological units. It is also able to reveal poor infiltration, reduced air exchange between the soil and the atmosphere	(Karnieli 1997).
The soil redness: RI	$RI = R^2/B * G^3$ (Mathieu et al. 1998)	Used as one of the indicators to evaluate the mineralogy of soils, including the iron content.	(Ray et al. 2014); (Escadafal and Huete 1991); (Mandal 2016).
The soil salinity: NDSI	$NDSI = (R - NIR) / (R + NIR)$ (Khan et al. 2005)	Is used to identify soils affected by salinity, and to show the spatial extent of salinity prevalent in our study area.	(Azabdaftari and Sunar 2016); (Chandana' et al. 2004); (Asfaw, et al, 2018); Gorji et al, 2015; Allbed et al, 2014; (Narmada, et al, 2015).

b. the soil indices

Escadafal and Huete 1991 use the soil color index to distinguish surface materials from soils according to the saturation of their color. Chikhaoui et al. 2005 characterize the state of land degradation in Morocco through the Land degradation index (LDI).

The following indices were therefore used in this study to highlight the mineralogical composition of soils, to assess the organic matter content of soils, and the physical state of soils in terms of moisture and compactness. Moreover, parameters such as color, brightness, texture, and moisture characterize the absorption properties of the soil constituents and are important for mapping soil conditions, particularly in arid environments.

The indices that characterize the soils using the reflectance curves and the spectral properties of the soil constituents (MSI, BI, crust Index, TI, cuirass Index, RI, color Index, GSI, NDSI). Cuirass and crust indices show that compact soils are mostly present in the southern part of the study area where soils are completely bare. The low values of the color index coincide with the high values of the redness index and correspond to the densely vegetated Lake Chad littoral spaces, which are therefore rich in organic matter. On the other hand, spaces with a low redness index have high values of brightness, MSI, and NDSI, which indicates low soil moisture and a prominent level of drought and soil salinity. Furthermore, in the southern part of the study area, where the levels of cuirass and crust are already high, the soil texture is also dominated by the presence of coarse particles considering the results of the texture indices and GSI

2.3.2. Statistical patterns

The model being developed also depends on the statistical information withdrawn from the indices. This includes linear regression, factor analysis, and principal component analysis were calculated.

a. linear regression

By adding all the indices used, we obtain a new image that summarizes all the information provided by each index. The image obtained will serve as the independent variable for the linear modeling between indices. The purpose is to highlight the potential regressions between the synthetic image of the indices used here as an explanatory variable, and each of the vegetation and soil indices used as variables to explain.

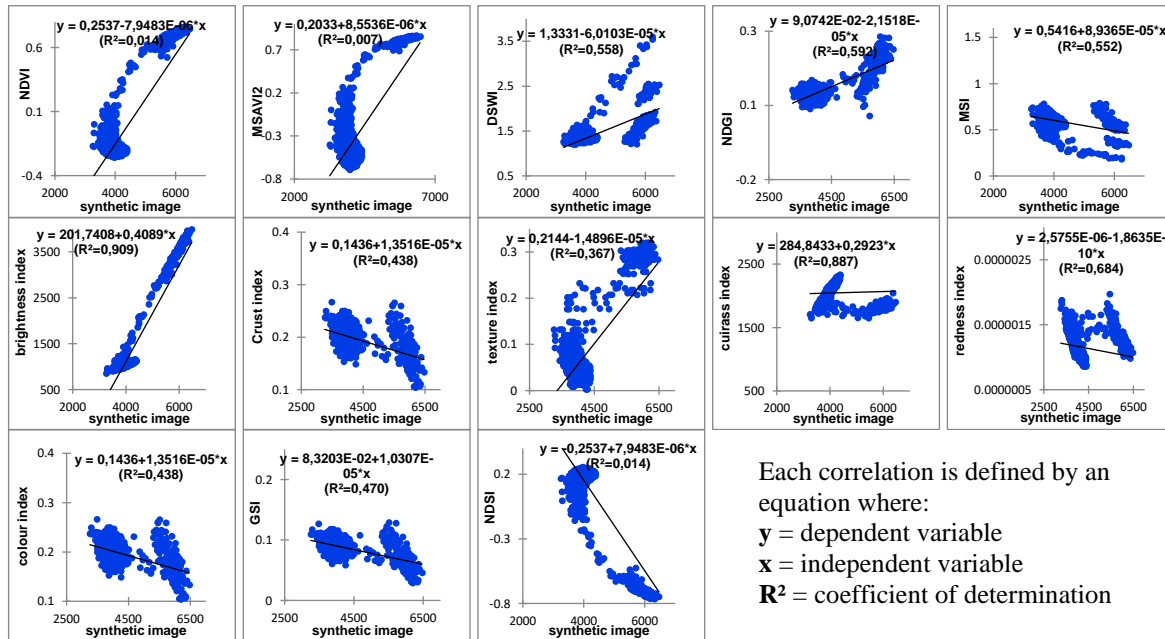


Figure 3: correlation between synthetic image and index's

It thus appears that five indices are negatively correlated to the synthetic image. These are the NDVI (-0.119), the DSWI (-0.747), NDGI (-0.769), TI (-0.606), and the redness index which has the most negative coefficient of correlation (-0.827). Moreover, the high values of the coefficient of determination of all the soil indices except the NDSI show their influence on the synthetic image (Table 3). The other correlations are positive with values

ranging from 0.119 for the NDSI to 0.953 for the brightness index.

The index most strongly determined by the synthesis image is the brightness index with an R^2 equal to 0.909. The other soil indices have an R^2 with values that vary in the interval [0.037-0.385]. For vegetation indices, the R^2 values are contained between 0.007 and 0.592.

Table 3: statistics relations between synthetic image and indices

Indices	Correlation Coefficient	Determination Coefficient	P values	
			Threshold	Test

NDVI	-0,119	$R^2=0,014$	$P < 0,0001$	Important
MSAVI2	0,081	$R^2=0,007$	$P < 0,0001$	Important
DSWI	-0,747	$R^2=0,558$	$P < 0,0001$	Important
NDGI	-0,769	$R^2=0,592$	$P < 0,0001$	Important
MSI	0,743	$R^2=0,552$	$P < 0,0001$	Important
BI	0,953	$R^2=0,909$	$P < 0,0001$	Important
Crust index	0,662	$R^2=0,438$	$P < 0,0001$	Important
TI	-0,606	$R^2=0,367$	$P < 0,0001$	Important
Cuirass index	0,942	$R^2=0,887$	$P < 0,0001$	Important
Redness index	-0,827	$R^2=0,684$	$P < 0,0001$	Important
Colour index	0,662	$R^2=0,438$	$P < 0,0001$	Important
GSI	0,685	$R^2=0,470$	$P < 0,0001$	Important
NDSI	0,119	$R^2=0,014$	$P < 0,0001$	Important

b. descriptive statistics

For this step, we use the factorial analysis which is a fundamental tool of statistical analysis of data tables that do not have a particular structure (Baccini 2010, Palm 1993). It is usually combined with the Principal Component Analysis (PCA) that is an extremely powerful tool for synthesizing information (Guerrien 2003), to reduce dimensional space (two for

example) to obtain the most relevant summary of the initial data. The output graphs are supported by characteristic numerical values, useful to ease the interpretation of the results. The graphs to be interpreted are, the geographical representations and the tables which make it possible to see the connections and the oppositions between the studied characteristics, according to the factors used for illustration.

Table 4: Factorial coordinates of indices

FACTORIAL ANALYSIS			PRINCIPAL COMPONENT ANALYSIS		
	F1	F2		F1	F2
NDVI	0,053	-0,976	NDVI	0,056	0,974
MSAVI2	-0,177	-0,960	MSAVI2	-0,172	0,961
DSWI	0,921	0,139	DSWI	0,927	-0,151
NDGI	0,964	0,159	NDGI	0,958	-0,169
MSI	-0,900	-0,075	MSI	-0,912	0,085
BI	-0,871	-0,133	BI	-0,889	0,143
Crust Index	-0,899	-0,203	Crust Index	-0,906	0,219
TI	0,581	-0,761	TI	0,584	0,764
Cuirass Index	-0,701	0,399	Cuirass Index	-0,731	-0,428
RI	0,641	-0,541	RI	0,664	0,574
Colour Index	-0,899	-0,203	Colour Index	-0,906	0,219
GSI	-0,922	-0,185	GSI	-0,925	0,198
NDSI	-0,053	0,976	NDSI	-0,056	-0,974

Factors “one” and “two” condense the most information and explain 85.62% of the common variability of the characteristics measured for the factor analysis and 87.54% for the PCA (Figure 4). Moreover, for each method, factor one with more than 54% of the information is more important than factor two that contains a little more than 31%. For each factor, the best-revealed indices are displayed in bold and the opposition of the indices is measured by the signs of the values (Table 4). For both methods, the first factor opposes DSWI, greenery, and redness indices, with MSI, brightness, crusting, cuirass, color, and GSI indices. On the second factor the NDVI, MSAVI2, and texture indices are opposed to the NDSI index. The degrees of opposition and their disposition are illustrated by the graph of correlations between variables and factors (Figure 4).

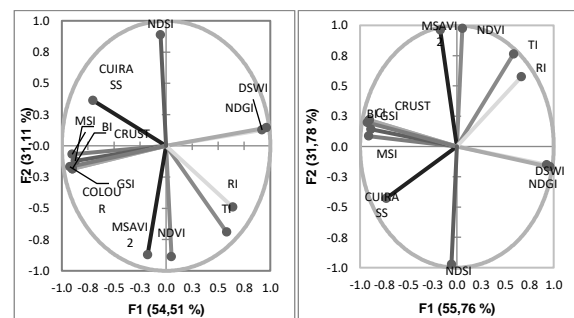


Figure 4: correlations between variables and factors

The symmetrical opposition of the first factor indices shows that in the studied area when the greenery is high and the DSWI is also high, the brightness and the crusting of the soils decrease, the

soils are wetter, darken, and the granulometry of topsoil is dominated by small particles. One can understand that the clear soils are much encrusted, dry, formed of particles of coarse size, and characterized by a high brightness. The correlation of the redness and texture indices with the four vegetation indices informs on the fact that red soils (hydromorphic and vertisol soils with significant iron content) and sandy soils are mostly present in the vegetated areas and as the soils are battleships vegetation cover decreases. Also, the opposition between NDVI and NDSI reflects the fact that the decline in chlorophyll activity is followed by an increase in soil salinity. Besides, the influence of soil salinity on plant quality and health is also observed by the proximity of NDSI with NDGI and DSWI in the correlation circle.

The first factor informs more about soil-related information and opposes five soil indices (MSI, BI, crust index, color index, GSI) to two vegetation indices, NDGI and the DSWI. Factor "two" concentrates vegetation information by contrasting the other two main vegetation indices (NDVI and MSAVI2) with the salinity index (NDSI). Consequently, the main characteristics of the soils derived from the correlations circles between indices (variables) and the factors are the organic matter content, humidity, and the physical state of the soils for the first factor. The second factor is the state and density of the vegetation cover.

However, the comparison of results obtained between the linear regression and the factorial analysis requires a few remarks. This concerns the

consistency of negative correlations between MSAVI2 and NDSI on one hand and positive correlations between MSAVI2 and NDVI on the other. Both are valid for linear regression and descriptive statistics and can then explain why the NDSI is not close to other soil indices. We notice the low representativeness of the cuirass, redness, and texture indices and their low correlation with the other indices. One can also note that in the correlation circle of the PCA, all the variables are far from the center than they are in the factorial's analysis one. The oppositions between the (variable) indices remain the same for the PCA as for the factorial analysis only their signs concerning the first-factor change.

2.3.3. The equation proposed for the model

The model's equation proposed here is designed to balance all the information obtained from the statistical analysis performed with the indices and based on previous work approaches. The adopted approach is to weigh the index maps with their coefficient of determination which serves us to highlight the individual contribution of each index to the final map of soil degradation. Also, we consider for each index of its highest values of factorial coordinates obtained through the factorial analysis and the PCA to preserve the best information provided by each of these methods of analysis. This information is combined to compose the following equation:

$$\text{ndvi}*(x_{\text{max}}+Y_{\text{max}})*R^2 + \text{msavi2}*(x_{\text{max}}+Y_{\text{max}})*R^2 + \text{dswi}*(x_{\text{max}}+Y_{\text{max}})*R^2 + \text{ndgi}*(x_{\text{max}}+Y_{\text{max}})*R^2 + \text{msi}*(x_{\text{max}}+Y_{\text{max}})*R^2 + \text{bi}*(x_{\text{max}}+Y_{\text{max}})*R^2 + \text{crust index}*(x_{\text{max}}+Y_{\text{max}})*R^2 + \text{ti}*(x_{\text{max}}+Y_{\text{max}})*R^2 + \text{cuirass index}*(x_{\text{max}}+Y_{\text{max}})*R^2 + \text{ri}*(x_{\text{max}}+Y_{\text{max}})*R^2 + \text{colour index}*(x_{\text{max}}+Y_{\text{max}})*R^2 + \text{gsi}*(x_{\text{max}}+Y_{\text{max}})*R^2 + \text{ndsi}*(x_{\text{max}}+Y_{\text{max}})*R^2 = \text{RISK OF SOILS DEGRADATION}$$

$$\text{ndvi}(17,09+0,64) 0,014 + \text{msavi2}(16,81+2,06) 0,007 + \text{dswi}(2,57+10,73) 0,558 + \text{ndgi}(2,88+11,23) 0,592 + \text{msi}(1,45+10,49) 0,552 + \text{bi}(2,44+10,23) 0,909 + \text{crust index}(3,73+10,47) 0,438 + \text{ti}(13,32+6,76) 0,367 + \text{cuirass index}(7,30+8,41) 0,887 + \text{ri}(9,79+7,46) 0,684 + \text{colour index}(3,73+10,47) 0,438 + \text{gsi}(3,23+10,74) 0,470 + \text{ndsi}(17,09+0,64) 0,014 = \text{RISK OF SOILS DEGRADATION}$$

3. RESULTS

3.1. Map of exposition soils degree to agents and degradation factors

The result of this modeling is a map of exposition soils degree to agents and degradation factors. The potential soil exposition state is classified on the map

below in five levels of exposition risk from the "Lower" level to the "Higher" (Table 5). The diversity of land cover explains the nature and the state of the soils, justifies the heterogeneity of the map, and explains the need to have a high number of classes to represent all the levels of exposition risk.

In the absence of field truth data, the different exposition levels are obtained by performing a standard deviation threshold of the image histogram. The standard deviation threshold method allows

visualizing how much the attribute values of a class vary compared to the mean, by using mean values and standard deviations from the mean.

Table 5: Classification of degradation levels

INDICES	EXPOSITIONS LEVELS				
	LOWER				HIGHER
NDVI (high to low chlorophyll activity)	0,501 - 0,861	0,285 - 0,501	0,070 - 0,285	-0,145 - 0,070	-0,502 - -0,145
MSAVI2 (high to low vegetation density)	0,425 - 0,925	0,041 - 0,425	-0,342 - 0,041	-0,726 - -0,342	-2,012 - -0,726
DSWI (high to low vegetation water stress)	1,516 - 6,787	1,252 - 1,516	0,988 - 1,252	0,724 - 0,988	0 - 0,724
NDGI (high to low vegetation greenery)	0,039 - 0,370	-0,040 - 0,039	-0,120 - -0,040	-0,200 - -0,120	-0,355 - -0,200
MSI (high to low soil moisture)	0 - 0,657	0,657 - 1,038	1,038 - 1,419	1,419 - 1,622	1,622 - 5,746
BI (low to high soil brightness)	0 - 1394,708	1394,708 - 3280,037	3280,037 - 5165,367	5165,367 - 7050,696	7050,696 - 15541,476
CRUST INDEX (low to high soil crusting)	-0,113 - 0,141	0,141 - 0,205	0,205 - 0,269	0,269 - 0,333	0,333 - 0,607
TI (low to high soil texture)	-0,578 - 0,007	0,007 - 0,078	0,078 - 0,149	0,149 - 0,220	0,220 - 0,428
CUIRASS INDEX (low to high soil cuirass)	-100 - 1703,341	1703,341 - 2439,784	2439,784 - 3176,226	3176,226 - 3912,669	3912,669061 - 366881
RI (high to low soils redness)	2,297e-006 - 1,403e-005	1,731e-006 - 2,297e-006	1,166e-006 - 1,731e-006	6,005e-007 - 1,166e-006	3,366e-009 - 6,005e-007
COLOR INDEX (low to high soil color)	304,098 - 833,117	833,117 - 1588,966	1588,966 - 2344,815	2344,815 - 3100,664	3100,664 - 16903,046
GSI (low to high grain size)	-0,085 - 0,042	0,042 - 0,088	0,088 - 0,133	0,133 - 0,189	0,189 - 0,416
NDSI (low to high soils salinity)	-0,861 - -0,506	-0,506 - -0,291	-0,291 - -0,075	-0,075 - 0,140	0,140 - 0,497

The "Lower" and "Moderate to low" levels cover the permanent open water areas of the lake, the marshland, and vegetated areas of the immediate shores, a portion of the intermediate shores, and occupy respectively 25,214.35 hectares and 130,717.19 hectares (Figure 5). The "Moderate" level of exposition spreads sparsely over the bare areas of the outer shores and the hinterland over an area of 137,404.34 hectares. The "High to moderate" and "Higher" levels dominate the outer shores and the hinterland. With 152,371.91 hectares, the "High to moderate" level represents the most widespread state of exposition of our study area. The "Higher" level occupies 29,175.73 hectares. The main difficulty now is to be able to identify for each level of exposition the most influential indices.

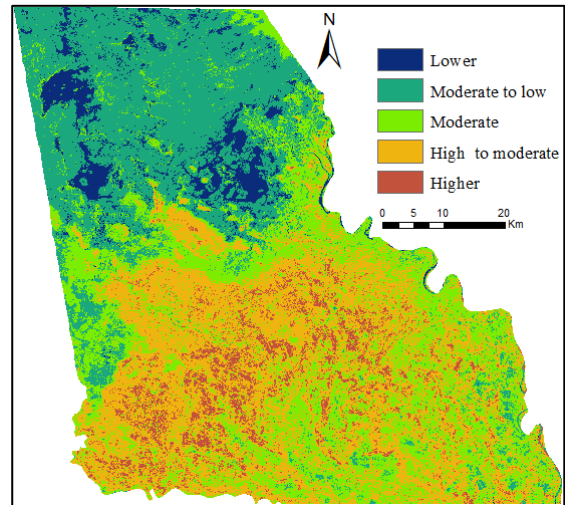


Figure 5: map of soils exposition risk to degradation

The method adopted to answer this concern is inspired by (Ngandam et al. 2016), which consists of classifying the indices by class of degradation and identifying the influence of the indices according to their spatial distribution by class (Table 6). For the "Higher" level, the top five indices with the largest spatial distributions are in decreasing order, DSWI (210,406.3 hectares), RI (168,640.87 hectares), GSI

(124,851.26 hectares), TI (62,076.68 hectares), and NDSI (41,903.57 hectares). As a result, the "Higher" level is explained by bare soils where vegetation has completely disappeared, the low rate of iron in the soil, the coarse texture of the surface particles, and high salinity. For the "High to moderate" level, the GSI, NDGI, RI, MSI, and crust index with respectively 227,054.85 hectares, 213,842.42 hectares, 196,491.09 hectares, 190,128.43 hectares, 179,840.75 hectares are the most indicative. This means that the soils of this class are also characterized by the coarse texture of the particles on the surface, but also by the weak greenery of the vegetation, an important crusting, and low moisture and iron contents.

The following indices: brightness (314,392.22 hectares), salinity (310,755.2 hectares), chlorophyll (310,022.07 hectares), crust (169,496.11 hectares) and cuirass (166,788.83 hectares) are the most influential for the "Moderate" level. The soils of this

class are clear and salty, weakly covered with vegetation, and compact on their surfaces.

A good vegetation cover of the soil, the fine texture of the soil particles, dark soils, weakly cuirassed, characterizes the "Moderate to low" level that covers the open waters of the lake, marshland areas, and part of the immediate and intermediate shores and which contain organic matter in significant quantities. Indeed, in this class, the MSAVI2 with 307,273.49 hectares is the most widespread index followed by TI 189,099.23 hectares, BI 131,856.39 hectares, cuirass index 114,273.9 hectares, and color index 103,409.8 hectares. In the "Lower" class, which occupies open water and marshland, the influence of vegetation indices is the most important (MSAVI2 116,895.5 hectares, NDGI 51,141.44 hectares, NDVI 47,347.15 hectares), the soil moisture is high (MSI 56,785.6 hectares), and their salinity rate is low (the NDSI 45,373.94 hectares).

Table 6: areas of degradation level by index.

LEVEL OF DEGRADATION	NDVI	MSAVI2	DSWI	NDGI	MSI	BI	CRUST INDEX	TI	CUIRASS INDEX	RI	COLOUR INDEX	GSI	NDSI
Lower	47347,15	116895,5	12232,53	51141,44	56785,6	20022,04	44050,68	436,12	34703,46	12455,87	42013,35	9303	45373,94
Moderate to low	65710,8	307273,49	43821,77	77454,57	73233,53	131856,39	75252,17	189099,23	114273,9	30834,54	103409,8	36286,48	66397,32
Moderate	310022,07	9348,34	65791,41	132378,86	122002,11	314392,22	169496,11	161940,13	166788,83	66436,07	134027,8	77362,84	310755,2
High to moderate	10351,48	15298,62	142606,5	213842,42	190128,43	8575,23	179840,75	61304,64	132939,34	196491,09	178548,4	227054,85	10428,33
Higher	41426,95	26042,49	210406,3	41,15	32708,78	15,46	6218,72	62076,68	26152,92	168640,87	16859,07	124851,26	41903,57
TOTAL	474858,45	474858,44	474858,5	474858,44	474858,45	474861,34	474858,43	474856,8	474858,45	474858,44	474858,4	474858,43	474858,4

3.2. Validation of results

A confusion matrix was used to validate the results obtained by a comparison with the existing map of the land degradation status of the far north region of Cameroon, provided by (Ngandam et al. 2016). A subset containing the main characteristic of the study area was used, i.e., the permanent open water, the marshland, the immediate shores, the external shores, and the hinterland.

So, the confusion matrix performed provided the information for verification and accuracy assessment between our results with the ground truth map. The overall accuracy which represents in percent the number of correctly classified values divided by the total numbers of values is 54.3%, and the kappa coefficient which assesses how much better the classification is than a random classification has a value of 40.49%.

4. CONCLUSION

The present work was based on laboratory tests applied to sentinel 2A satellite images. The purpose was to model the risk of soil degradation in Sahelian regions by combining spectral indices with statistical analyses. The results are highly correlated to some factors as the phenological season of satellite image acquisition, the quality of the images, the formula of the indices used, and the applied statistical treatments.

Also, statistical analysis was applied to the resulting image giving on one hand the correlation and determination coefficients of each index, and on the other hand, the factorial axes which summarize more information. All indices are considered statistically significant (P-value < 0.0001). The first two factors of PCA and factorial analysis explain respectively 87.54 % and 85.62 % of the common variability of the characteristics measured. The first factor contains the soil information, and the second factor focuses information on vegetation. This final equation of the model is obtained by index weighting with the respective values of the coefficient of determination, which oscillates between 0.007 for the MSAVI2 and 0.909 for the brightness index. Among

the most serious levels of degradation, the "High to moderate" level is the most widespread with 15,271.91 hectares, followed by the "Moderate" level with 137,404.34 hectares, and the "Higher" level, which occupies an area of 29,175.73 hectares.

However, we apply our methodology to images of a specific month of the year (April). So, the challenge now is the adaptation of the model to previous years and other periods of the year. Moreover, the lack of consideration of urban areas is a limit for this work because the elements that constitute the habitat (example of aluminum roofs) necessarily influence the results of the calculation of certain indices.

At last, whatever performing decorrelation analysis as a method of unlinking indices, all of them is calculated on satellite images from the same sensor. Consequently, they have a basic dependent relation because of their origin same spectral characteristics. For this reason, it should be interesting in further analysis to perform the whole analysis on multisource satellite images (SPOT or MODIS), to assess the statistic behavior and decorrelation, while an index of one source and another of the other source is used as the independent and dependent variable.

Moreover, the method adopted in this study to evaluate the contribution of the different indices to each degree of degradation brought interesting results. However, the presence on our images of open waters and marshland to a certain extent brings out a new constraint to consider. The low values of vegetation indices of NDVI and MSAVI2 appear in open water rather than appearing in bare spaces. Without this class of occupation, these two indices would have better contributed to characterize the classes of strong degradation as the DSWI did. To overcome this difficulty, one of the ways of improving the model will be to classify indices as functions of the distinct levels of degradation, using the spectral windows obtained from the spectral signature of these indices.

The imbalance between the number of vegetation index and the number of soil index is to be considered, through a readjustment that will allow integrating new parameters including climatic like the temperature of the surface, precipitations, albedo, or evapotranspiration. Other elements such as topography and hydrographic network distribution are also to be considered.

ACKNOWLEDGMENTS

The authors are grateful to European Space Agency (ESA) and the Copernicus program for the Sentinel 2

satellite images direct access. We thank all those who contributed to this article.

REFERENCES

- Ali, Faleh, and Bouhlassa Saïdati. 2003. 'Exploitation Des Mesures Magnétiques Dans l'étude de l'état de Stabilité Des Sols: Cas Des Bassins-Versants Abdelali et Markat (Prérif-Maroc)'. *Papeles de Geografía*, 14.
- Allbed, Amal, Lalit Kumar, and Yousef Y. Aldakheel. 2014. 'Assessing Soil Salinity Using Soil Salinity and Vegetation Indices Derived from IKONOS High-Spatial Resolution Imageries: Applications in a Date Palm Dominated Region'. *Geoderma* 230–231 (October): 1–8.
- Apan, Armando, Alex Held, Stuart Phinn, and John Markley. 2003. 'Formulation and Assessment of Narrow-Band Vegetation Indices from EO-1 Hyperion Imagery for Discriminating Sugarcane Disease', 13.
- Asfaw, Engdawork, K. V. Suryabagavan, and Mekuria Argaw. 2018. 'Soil Salinity Modeling and Mapping Using Remote Sensing and GIS: The Case of Wonji Sugar Cane Irrigation Farm, Ethiopia'. *Journal of the Saudi Society of Agricultural Sciences* 17 (3): 250–58.
- Azabdaftari, A., and F. Sunar. 2016. 'Soil Salinity Mapping Using Multitemporal Landsat Data'. *ISPRS - International Archives of the Photogrammetry, Remote Sensing and Spatial Information Sciences* XLI-B7 (June): 3–9.
- Baccini, Alain. 2010. 'Statistique Descriptive Multidimensionnelle'.
- Bannari, A., A. R. Huete, D. Morin, and F. Zagolski. 1996. 'Effets de La Couleur et de La Brilliance Du Sol Sur Les Indices de Végétation'. *International Journal of Remote Sensing* 17 (10): 1885–1906.
- Caloz, Régis, and Claude Collet. 2011. *Précis de Télédétection Volume 3 Traitements Numériques d'images de Télédétection*. Vol. 3. Presses de l'Université du Québec.
- Chamard, Ph.C, M.C Guenegou, Jeannine Lerhun, J. Levasseur, and M. Togola. 1991. 'Utilisation Des Bandes Spectrales Du Vert et Du Rouge Pour Une Meilleure Évaluation Des Formations Végétales Actives'. In *Congrès AUPELF-UREF*, edited by Marie-Françoise Courel, 6. Sherbrooke, Canada.
- Chandana, PG, K D N Weerasinghe, S Subasinghe, and S Pathirana. 2004. 'Remote Sensing Approach to Identify Salt-Affected Soils in Hambantota District', 6.
- Chen, Di, Naijie Chang, Jingfeng Xiao, Qingbo Zhou, and Wenbin Wu. 2019. 'Mapping Dynamics of Soil Organic Matter in Croplands with MODIS Data and Machine Learning Algorithms'. *Science of The Total Environment* 669 (June): 844–55.
- Chikhaoui, Mohamed, Ferdinand Bonn, Amadou Idrissa Bokoye, and Abdelaziz Merzouk. 2005. 'A Spectral Index for Land Degradation Mapping Using ASTER Data: Application to a Semi-Arid Mediterranean

- Catchment'. *International Journal of Applied Earth Observation and Geoinformation* 7 (2): 140–53.
- Chikhaoui, Mohamed, Ferdinand Bonn, Abdelaziz Merzouk, and Bernard Lacaze. 2007. 'Cartographie de La Dégradation Des Sols à l'aide Des Approches Du Spectral Angle Mapper et Des Indices Spectraux En Utilisant Des Données Aster'. *Revue Télédétection* 7 (1-2-3-4): 343–57.
- Eklundh, Lars, and Lennart Olsson. 2003. 'Vegetation Index Trends for the African Sahel 1982–1999'. *Geophysical Research Letters* 30 (8).
- Elhag, Mohamed, and Jarbou A. Bahrawi. 2017. 'Soil Salinity Mapping and Hydrological Drought Indices Assessment in Arid Environments Based on Remote Sensing Techniques'. *Geoscientific Instrumentation, Methods and Data Systems* 6 (1): 149–58.
- Escadafal, Richard, and A. Huete. 1991. 'Etude des propriétés spectrales des sols arides appliquée à l'amélioration des indices de végétation obtenus par télédétection'. *Comptes Rendus de l'Académie des Sciences.Série 2 : Mécanique...* 312: 1385–91.
- Farooq Ahmad. 2012. 'Spectral Vegetation Indices Performance Evaluated for Cholistan Desert'. *Journal of Geography and Regional Planning* 5 (6).
- Gao, Yongnian, Junfeng Gao, Jing Wang, Shuangshuang Wang, Qin Li, Shuhua Zhai, and Ya Zhou. 2017. 'Estimating the Biomass of Unevenly Distributed Aquatic Vegetation in a Lake Using the Normalized Water-Adjusted Vegetation Index and Scale Transformation Method'. *Science of The Total Environment* 601–602 (December): 998–1007.
- Gbetkom, Paul Gérard, Sébastien Gadal, Ahmed El Aboudi, Alfred Homère Ngandam Mfondoum, and Mamane Barkawi Mansour Badamassi. 2018. 'Mapping Change Detection of LULC on the Cameroonian Shores of Lake Chad and Its Hinterland through an Inter-Seasonal and Multisensor Approach'. *International Journal of Advanced Remote Sensing and GIS* 7 (1): 2835–49.
- Gérard Begni, Richard Escadafal, Delphine Fontannaz, and Anne-Thérèse Hong-Nga Nguyen. 2005. 'La Télédétection : Un Outil Pour Le Suivi et l'évaluation de La Désertification', no. 2: 48.
- GIZ. 2015. 'Audit Environnemental Conjoint Sur l'Assèchement Du Lac Tchad'. Afrique du Sud.
- Gorji, Taha, Aysegul Tanik, and Elif Sertel. 2015. 'Soil Salinity Prediction, Monitoring and Mapping Using Modern Technologies'. *Procedia Earth and Planetary Science* 15: 507–12.
- Guerrien, Marc. 2003. 'L'intérêt de l'analyse En Composantes Principales (ACP) Pour La Recherche En Sciences Sociales: Présentation à Partir d'une Étude Sur Le Mexique'. *Cahiers Des Amériques Latines*, no. 43 (July): 181–92.
- Houssa, Rachida, Jean-Claude Pion, and Hervé Yésou. 1996. 'Effects of Granulometric and Mineralogical Composition on Spectral Reflectance of Soils in a Sahelian Area'. *ISPRS Journal of Photogrammetry and Remote Sensing* 51 (6): 284–98.
- Jazouli, Aafaf El, Ahmed Barakat, Rida Khellouk, Jamila Rais, and Mohamed El Baghdadi. 2019. 'Remote Sensing and GIS Techniques for Prediction of Land Use Land Cover Change Effects on Soil Erosion in the High Basin of the Oum Er Rbia River (Morocco)'. *Remote Sensing Applications: Society and Environment* 13 (January): 361–74.
- Karnieli, A. 1997. 'Development and Implementation of Spectral Crust Index over Dune Sands'. *International Journal of Remote Sensing* 18 (6): 1207–20.
- Kauth, R., and G. Thomas. 1976. 'The Tasseled Cap -- A Graphic Description of the Spectral-Temporal Development of Agricultural Crops as Seen by LANDSAT'. *LARS Symposia*, January.
- Khan, Nasir M., Victor V. Rastokuev, Y. Sato, and S. Shiozawa. 2005. 'Assessment of Hydrosaline Land Degradation by Using a Simple Approach of Remote Sensing Indicators'. *Agricultural Water Management* 77 (1–3): 96–109.
- Li, Heli, Chunjiang Zhao, Guijun Yang, and Haikuan Feng. 2015. 'Variations in Crop Variables within Wheat Canopies and Responses of Canopy Spectral Characteristics and Derived Vegetation Indices to Different Vertical Leaf Layers and Spikes'. *Remote Sensing of Environment* 169 (November): 358–74.
- Li, Xinchuan, Youjing Zhang, Yansong Bao, Juhua Luo, Xiuliang Jin, Xingang Xu, Xiaoyu Song, and Guijun Yang. 2014. 'Exploring the Best Hyperspectral Features for LAI Estimation Using Partial Least Squares Regression'. *Remote Sensing* 6 (7): 6221–41.
- Madeira Netto, José. 1991. 'Etude quantitative des relations constituants minéralogiques-réflectance diffuse des latosols brésiliens: application à l'utilisation pédologique des données satellitaires TM (région de Brasilia)'. Bondy: ORSTOM. Centre IRD de Bondy.
- Maimouni, S., A. Bannari, A. El-Harti, and A. El-Ghmari. 2011. 'Potentiels et limites des indices spectraux pour caractériser la dégradation des sols en milieu semi-aride'. *Canadian Journal of Remote Sensing* 37 (3): 285–301.
- Maimouni, Soufiane, and Abderrazak Bannari. 2011. 'Cartographie de La Dégradation Des Sols En Milieu Semi-Aride', 10.
- Mandal, Umesh K. 2016. 'Spectral Color Indices Based Geospatial Modeling of Soil Organic Matter in Chitwan District, Nepal'. *ISPRS - International Archives of the Photogrammetry, Remote Sensing and Spatial Information Sciences* XLI-B2 (June): 43–48.
- Martín-Sotoca, Juan J., Antonio Saa-Requejo, Javier Borondo, and Ana M. Tarquis. 2018. 'Singularity Maps Applied to a Vegetation Index'. *Biosystems Engineering* 168 (April): 42–53.
- Mathieu, Renaud, Marcel Pouget, Bernard Cervelle, and Richard Escadafal. 1998. 'Relationships between Satellite-Based Radiometric Indices Simulated Using Laboratory Reflectance Data and Typic Soil Color of an Arid Environment'. *Remote Sensing of Environment* 66 (1): 17–28.
- Narmada, Gobinath, and Bhaskaran. 2015. 'Monitoring and Evaluation of Soil Salinity in Terms of Spectral

- Response Using Geoinformatics in Cuddalore Environs'. *International Journal of Geomatics and Geosciences* 5 (4): 536–43.
- Ngandam, Mfondoum Alfred Homère, Joachim Etouna, Buji Kindess Nongsi, Fabrice Armel Mvogo Moto, and Florine Gustave Noulakoupe Deussieu. 2016. 'Assessment of Land Degradation Status and Its Impact in Arid and Semi-Arid Areas by Correlating Spectral and Principal Component Analysis Neo-Bands'. *International Journal of Advanced Remote Sensing and GIS* 5 (1): 1539–60.
- Okaingni, Jean-Claude, Koffi Fernand Kouamé, and Arnaud Martin. 2010. 'Cartographie Des Cuirasses Dans Les Formations Volcano- Sédimentaires de La Zone d'anikro- Kadiokro (Côte d'Ivoire) à l'aide de La Théorie Des Fonctions de Croyance'. *Revue Télédétection* 9 (1): 19–32.
- Oliveira, Pedro D. de, Michel K. Sato, Sueli Rodrigues, and Herdjanía V. de Lima. 2016. 'S-Index and Soybean Root Growth in Different Soil Textural Classes'. *Revista Brasileira de Engenharia Agrícola e Ambiental* 20 (4): 329–36.
- Palm, R. 1993. 'Les Méthodes d'analyse Factorielle : Principes et Applications', 36.
- Pandey, Prem Chandra, Meenu Rani, Prashant Kumar Srivastava, Laxmi Kant Sharma, and Mahendra Singh Nathawat. 2013. 'Land Degradation Severity Assessment with Sand Encroachment in an Ecologically Fragile Arid Environment: A Geospatial Perspective'. *QScience Connect*, no. 2013 (March): 43.
- Pang, Guojin, Xuejia Wang, and Meixue Yang. 2017. 'Using the NDVI to Identify Variations in, and Responses of, Vegetation to Climate Change on the Tibetan Plateau from 1982 to 2012'. *Quaternary International* 444 (July): 87–96.
- 'Plan d'Action National de Lutte Contre La Désertification (PAN/LCD)'. 2006.
- Pouchin, T. 2001. 'Cours de Télédétection'. Université Le Havre France.
- Pu, R. 2008. 'An Exploratory Analysis of in Situ Hyperspectral Data for Broadleaf Species Recognition', 6.
- Qi, J., A. Chehbouni, A.R. Huete, Y.H. Kerr, and S. Sorooshian. 1994. 'A Modified Soil Adjusted Vegetation Index'. *Remote Sensing of Environment* 48 (2): 119–26.
- Rallo, Giovanni, Mario Minacapilli, Giuseppe Ciraolo, and Giuseppe Provenzano. 2014. 'Detecting Crop Water Status in Mature Olive Groves Using Vegetation Spectral Measurements'. *Biosystems Engineering* 128 (December): 52–68.
- Ray, S S, J P Singh, Gargi Das, and Sushma Panigrahy. 2014. 'Use of High Resolution Remote Sensing Data for Generating Site-Specific Soil Management Plan', 6.
- Renard, K. G., G. R. Foster, G. A. Weesies, D. K. McCool, and D. C. Yoder. 1997. *Predicting Soil Erosion by Water: A Guide to Conservation Planning with the Revised Universal Soil Loss Equation (RUSLE)*. US Government Printing Office.
- Romero, Maria, Yuchen Luo, Baofeng Su, and Sigfredo Fuentes. 2018. 'Vineyard Water Status Estimation Using Multispectral Imagery from an UAV Platform and Machine Learning Algorithms for Irrigation Scheduling Management'. *Computers and Electronics in Agriculture* 147 (April): 109–17.
- Rouse, John Wilson, R. H. Haas, John A. Schell, and Donald W. Deering. 1973. 'Monitoring Vegetation Systems in the Great Plains with ERTS', 309–17.
- Seignobos, Christian, and Olivier Iyébi-Mandjek. 2000. 'Atlas de la province Extrême-Nord Cameroun'. Paris : Yaoundé: Institut de recherche pour le développement ; République de Cameroun, Ministère de la recherche scientifique et technique, Institut national de cartographie.
- StéphaneKoff, Avy, Abderrahman Ait Fora, and Hicham Elbelrhiti. 2016. 'Cartographie de l'état Du Couvert Végétal Du Nord de La Côte d'Ivoire à Partir d'images Satellites: Exemple de La Zone de Korhogo'. *European Scientific Journal, ESJ* 12 (29): 204.
- Sun, Hong, Minzan Li, and Daoliang Li. 2011. 'The Vegetation Classification in Coal Mine Overburden Dump Using Canopy Spectral Reflectance'. *Computers and Electronics in Agriculture* 75 (1): 176–80.
- Symeonakis, E., and N. Drake. 2004. 'Monitoring Desertification and Land Degradation over Sub-Saharan Africa'. *International Journal of Remote Sensing* 25 (3): 573–92.
- Symeonakis, Elias, and Nick Drake. 2010. '10-Daily Soil Erosion Modelling over Sub-Saharan Africa'. *Environmental Monitoring and Assessment* 161 (1–4): 369–87.
- Welikhe, Pauline, Joseph Essamua Quansah, Souleymane Fall, and Wendell McElhenney. 2017. 'Estimation of Soil Moisture Percentage Using LANDSAT-Based Moisture Stress Index'. *Journal of Remote Sensing & GIS* 06 (02).
- Wischmeier, Walter H., and Dwight David Smith. 1978. *Predicting Rainfall Erosion Losses: A Guide to Conservation Planning*. Department of Agriculture, Science and Education Administration.
- Xiao, J., Y. Shen, R. Tateishi, and W. Bayaer. 2006. 'Development of Topsoil Grain Size Index for Monitoring Desertification in Arid Land Using Remote Sensing'. *International Journal of Remote Sensing* 27 (12): 2411–22.
- Xiao, Jieying, Yanjun Shen, and Tateishi Ryutaro. 2014. 'Mapping Soil Degradation by Topsoil Grain Size Using MODIS Data', 8.
- Yongnian Zeng, Zhaodong Feng, and Nanping Xiang. 2004. 'Assessment of Soil Moisture Using Landsat ETM+ Temperature/Vegetation Index in Semiarid Environment'. In *IEEE International IEEE International Geoscience and Remote Sensing Symposium, 2004. IGARSS '04. Proceedings. 2004*, 6:4306–9. Anchorage, AK, USA: IEEE.